JOURNAL OF AIRCRAFT
Vol. 41, No. 5, September–October 2004

Effects of Surface Finish on Aerodynamic Performance of a Sailboat Centerboard

David S. Miklosovic,* Michael P. Schultz,† and Christian Esquivel‡
United States Naval Academy, Annapolis, Maryland 21402

A centerboard stabilizer from a Laser™ sailboat was wind-tunnel tested at different surface finish conditions to ascertain the effects on performance. The stabilizer model had an NACA 0009 airfoil section, an aspect ratio of 1.8, and a leading-edge sweep angle of 22 deg. Tests were run at Reynolds numbers of 5.6×10^5 and 1.06×10^6, based on the mean aerodynamic chord. Surface finishes of 0.04–0.46 mils (1.0–11.6 μm) rms roughness height were generated by sanding with different grit abrasives and quantified using surface laser scanning techniques. The effects of progressively "improving" the surface finish of the lifting surface (e.g., by sanding and polishing) demonstrated the potential to decrease the maximum lift coefficient (15%), increase the drag coefficient at equivalent lift coefficient (138%), and invert the magnitude of the pitching moment coefficient (a 167% decrease). The combination of the roughest surface finishes at the higher Reynolds number delayed flow separation to higher angles of attack and qualitatively changed the stall characteristics, resulting in generally superior performance over the smooth surface conditions. These results indicate that polishing reduces the overall performance of sailboat stabilizers at these Reynolds numbers, and these decrements can impact the practical operating envelope. However, applicability of these results to aircraft control surfaces is limited because the range of effect is outside the typical operating envelope.

Nomenclature

AR = wing aspect ratio, b^2/S
a = lift-curve slope, $\dfrac{dC_L}{d\alpha}$
b = wing span
C_D = wing drag coefficient, $D/\frac{1}{2}\rho U_\infty^2 S$
C_{D_i} = induced drag coefficient, $C_L^2/\pi ARe$
$C_{D_{\min}}$ = minimum drag coefficient
C_{D_0} = drag coefficient at zero lift
C_L = wing lift coefficient, $L/\frac{1}{2}\rho U_\infty^2 S$
C_{L_m} = lift coefficient at minimum drag coefficient
C_m = wing pitching-moment coefficient, $M/\frac{1}{2}\rho U_\infty^2 S\bar{c}$
C_{m_0} = pitching-moment coefficient at zero lift
$\bar{c}$ = wing mean chord, also MAC
D = wing drag force
e = span efficiency factor, $1/1+\delta$
L = wing lift force
L/D = aerodynamic efficiency
M = wing pitching moment
MAC = wing mean aerodynamic chord, also $\bar{c}$
R_a = centerline average roughness height, $\dfrac{1}{N}\sum_{i=1}^{N}|y_i|$
R_q = rms roughness height, $\sqrt{\dfrac{1}{N}\sum_{i=1}^{N}y_i^2}$
R_t = maximum peak to trough roughness height, $y_{\max} - y_{\min}$
R_z = 10-point roughness height, $\dfrac{1}{5}\sum_{i=1}^{5}(y_{\max i} - y_{\min i})$
Re = Reynolds number, $U_\infty\bar{c}/\nu$
S = wing planform area, $b\bar{c}$
U_∞ = freestream velocity
y = wall-normal distance from surface datum
α = angle of attack
α_{L_0} = angle of attack at zero lift
δ = Glauert spanwise loading correction factor
ν = kinematic viscosity
ρ = fluid density

Received 13 February 2003; revision received 7 July 2003; accepted for publication 30 July 2003.

*Assistant Professor, Aerospace Engineering Department. Member AIAA.
†Assistant Professor, Naval Architecture and Ocean Engineering Department.
‡Ensign, United States Naval Reserve.

Introduction

A SIGNIFICANT number of engineering applications involve flows that develop over surfaces that are rough to varying degree. Even surfaces that are hydraulically smooth at low unit Reynolds number can be considered rough at higher unit Reynolds number. (Hydraulically smooth is defined as a surface quality that exhibits no effects of decreasing skin friction with decreasing roughness height.) In many cases the roughness is the result of the surface finish produced by the painting, sanding, or polishing process. Examples range from wing and airfoil/hydrofoil models prepared for wind- and water-tunnel testing to full-scale aircraft stabilizers, sailing hulls, keels, and rudders. Particularly in the application of dinghy sailing, there exists a commonly held belief that polishing the centerboard or daggerboard will improve the keel performance. Although studies of the effect of locally applied roughness on lifting surfaces have been well reported, particularly in the area of leading-edge excrescence, there is a paucity of data that documents the effect of systematic changes in the surface finish quality on the aerodynamic performance of lifting surfaces. The objective of the present investigation is to document the experimental variation in aerodynamic performance of a sailboat stabilizer model with surface finishes produced by sanding and polishing. The surface finish quality, less than 0.46 mils (11.6 μm) rms roughness height, was scanned and statistically quantified for each case. Thus, the present work represents a scale and a degree of systematic documentation of the surface quality not previously reported.

Several previous studies have focused on surface roughness effects on flow over airfoils and wings. Abdel-Rahman and Chakroun[1] conducted an experimental investigation of the effect of sandpaper roughness on the lift and drag of a NACA 0012 airfoil at $Re = 1.7 \times 10^5$ to 3.4×10^5. Their results indicated a trend that C_{D_0} increased with increasing scale of roughness. The roughness was also shown to delay separation and to increase C_L in the stall region. Roughness decreased the maximum L/D as much as 55%. However, the angle of attack at which maximum L/D occurred was unchanged. Chakroun et al.[2] carried out an experimental study of a NACA 2412 airfoil with a flap covered with sandpaper roughness at a Reynolds number of 3.3×10^5. At a zero flap angle a reduction in both the lift and drag was observed with increasing roughness. However, the maximum L/D increased with increasing roughness. Mueller and Batill[3] performed an experimental study of a NACA 66_3-018 airfoil with grit roughness attached to the leading edge at $Re = 4.0 \times 10^4$ to 4.0×10^5. The roughness was noted to have a similar effect to a laminar leading-edge separation bubble, which promotes transition and turbulent reattachment.

The effect of accumulated excrescence as a result of the impact of insects on wind-turbine airfoils has been studied in the last decade. Gregorek[4] presented experimental results for NACA 23015, S-809, and SANDIA 0018/50 airfoil sections. Even moderate simulated contamination yielded a 10% reduction in $C_{L_{\max}}$, a 60% increase in C_{D_0}, and a 33% change in pitching-moment coefficient. Moreover, the lift-curve slope decreased by 20% as a result of added excrescence. Similar studies by Reuss et al.[5] were repeated for NACA 4415 and LS(1)-0417MOD airfoil sections. These experiments resulted in a 30% reduction in $C_{L_{\max}}$ and an increase in C_{D_0} greater than 60%.

Another reason for interest in surface roughness effects on wings arises from the need to predict aerodynamic performance in icing conditions. Wickens and Nguyen[6] conducted an experimental study of a wing-propeller model with a distributed roughness on the upper surface to simulate ice accretion. They found that the roughness reduced both the lift-curve slope and the maximum lift of the wing. Their results also showed that the leading-edge region was especially sensitive to the roughness. Removal of the roughness near the leading edge returned the wing performance to nearly its original state. A recent review of computational and experimental studies on wing icing is given by Kind et al.[7]

Studies have also been conducted to determine the effects of surface finish on the performance of gas-turbine airfoils.[8,9] These studies concentrated on compressible flow regimes at much higher Reynolds numbers.

A large body of basic research has focused on the effect of surface roughness on turbulent boundary-layer structure and frictional resistance (e.g., Refs. 10–16). Although a great deal of data has been generated for canonical roughness patterns (i.e., uniform sand,[10] two-dimensional transverse ribs,[11] and expanded mesh on the wall boundary[12]), studies involving naturally occurring roughness (e.g., rime ice accretion, insect contamination, and environmentally induced surface erosion) are much less numerous. Recently, Song and Eaton[17] experimentally studied a turbulent boundary layer developing over a sandpaper rough wall subjected to a strong adverse pressure gradient. Their results showed that the roughness led to earlier separation and increased the length of the separation bubble compared to the smooth wall case.

Schultz[18] used towing tank tests to document the frictional resistance of sanded and polished surfaces on a flat plate. These results indicated an increase in the frictional resistance coefficient of up to 7.3% for an unsanded, as-sprayed paint surface compared to a sanded, polished surface. Significant increases in the frictional resistance coefficient were also noted on surfaces sanded with sandpaper as fine as 600 grit as compared to the polished surface. Bethwaite[19] tested sailboat rudders having NACA 0009 sections. Field tests indicated a 23% increase in lift at a fixed angle of attack for a 1200-grit sanded and polished rudder vs a 1200-grit sanded, unpolished rudder. Unfortunately, the experimental conditions for the tests were not well documented.

Experimental Apparatus

The present tests were performed in the Closed-Circuit Wind Tunnel (CCWT), an incompressible flow facility at the U.S. Naval Academy. Tests are accomplished in the vented test section, which has a cross section of 54 × 38 in. (137 × 97 cm) and a length of 94 in. (239 cm). The contraction ratio is 6.23, and the resulting tunnel turbulence factor is 1.073. Semispan wing models are positioned just above a wall boundary-layer splitter plate/reflection plane with a typical clearance of 0.070 in. (1.8 mm), as shown in Fig. 1. The splitter plate is offset 2.75 in. (6.99 cm) from the tunnel floor. The maximum Reynolds number achievable in this facility is 1.4×10^6 per foot (4.6×10^6 per meter).

Instrumentation

Aerodynamic forces and moments are transmitted to a six-component external compact platform balance located beneath the test-section yaw table. The standard deviation in force measurement over a representative 15-min test at a constant flow condition has been demonstrated to be ±0.03 lb (0.13 N) in drag, ±0.24 lb (1.08 N) in lift, and ±0.08 ft-lb (0.11 Nm) in pitching moment. The coefficients for these forces have standard deviations of ±0.0003, ±0.003, and ±0.001, respectively, for the present wind-tunnel model. Additionally, the test section is instrumented with pressure transducers and a thermocouple to obtain real-time measurement of flow velocity and air density. Steady-state signals are measured using a $6\frac{1}{2}$-digit multiplexer/data logger.

Wing Model Configuration

The wing half-model used was a modified centerboard from a Laser™ sailboat. This geometry represents a typical sailing craft stabilizer and was constructed of a high-density foam core reinforced with stainless wire stiffeners and two aluminum spars and was surfaced with polyamide epoxy. The model has a constant-chord symmetric NACA 0009 airfoil section with a moderate sweep angle of 22 deg, a chord of 14.00 in. (35.56 cm), and a semispan of 25.00 in. (63.50 cm). Thus, the reference area is 2.431 ft^2 (2258.1 cm^2), and the aspect ratio is 1.786 (an effective aspect ratio of 3.571).

A single wing model with seven different surface finishes was used for all of the present experiments. This was done to ensure that any measured differences in the aerodynamic performance were

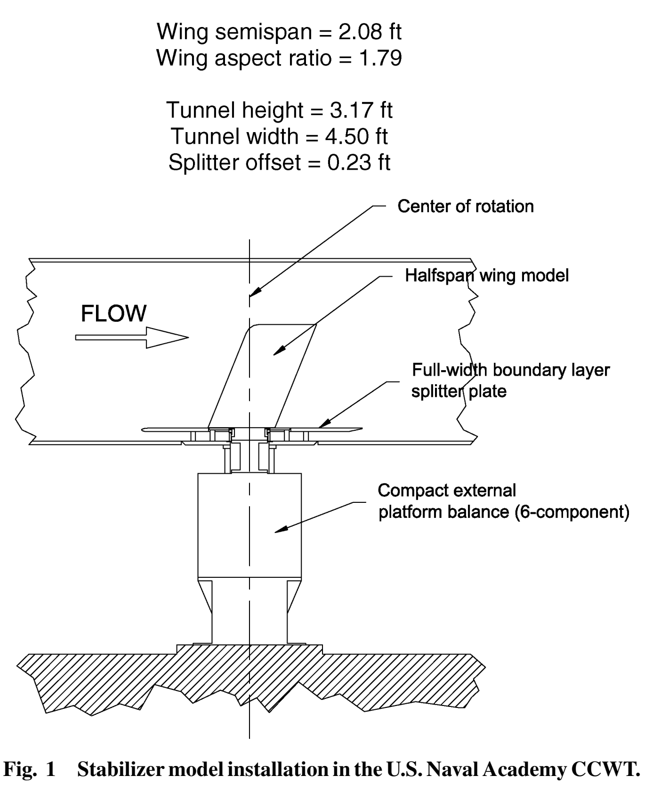

Fig. 1 Stabilizer model installation in the U.S. Naval Academy CCWT.

caused by the surface condition of the wing and not a result of geometry variations from the fabrication process. The tested surface finishes were the same as tested by Schultz[18] in flat-plate frictional resistance experiments. The wing was initially painted with several coats of polyamide epoxy paint manufactured by International Paint. This surface condition was termed the unsanded or as-sprayed condition and represented the roughest surface measured with visible "orange peel" patterns in the paint. After aerodynamic testing the wing was wet sanded with 60-grit sandpaper. This surface was referred to as the 60-grit sanded condition. Subsequent to aerodynamic testing under the 60-grit sanded condition, the entire process was repeated for the 120-grit sanded, 220-grit sanded, 400-grit sanded, and 600-grit sanded surface conditions. After aerodynamic testing of the 600-grit sanded surface, the wing was wet sanded up to 1800 grit and polished with a buffing wheel using Meguiar's swirl remover polishing compound. This surface is referred to as the polished condition. Great care was taken to ensure that the entire wetted area was uniformly sanded with each abrasive grit.

Roughness Characteristics

The surface finish of the wing model was measured using a laser diode point range sensor laser profilometer system mounted to a two-axis traverse with a resolution of 0.20 mils (5 μm). The resolution of the sensor is 0.04 mils (1 μm) with a laser spot diameter of 0.39 mils (10 μm). Data were taken over a sampling length of 1.97 in. (50 mm) and were digitized at a sampling interval of 1 mil (25 μm). Ten linear profiles were taken on each of the test surfaces. A single three-dimensional topographic profile was performed on each of the surfaces by sampling over a square area 0.2 in. (5 mm) on a side with a sampling interval of 1 mil (25 μm). Examples of these topographic profiles are presented for the 60-grit and 120-grit sanded specimens in Figs. 2 and 3. The roughness statistics presented herein were calculated using the linear profiles from each of the seven surface finishes and are summarized in the roughness plot of Fig. 4.

Experimental Procedure and Data Reduction/Corrections

The experiments were conducted at Reynolds numbers of 5.6×10^5 and 1.06×10^6 as referenced to the freestream velocity and $\bar{c}$ and corrected for the tunnel turbulence factor. For each surface finish the model was rotated through a pitch sweep of -5 to $+15$ deg in 1-deg increments using the pitch-pause technique. Approximately 5 s were allocated for tunnel transients to diminish prior to triggering the data-acquisition system.

The acquired raw force data were reduced to coefficient form and corrected for wall-interference effects in accordance with the standard procedures outlined in Barlow et al.[20] The corrected results are presented herein. In general, the most conservative estimates for horizontal buoyancy effects yielded a 0.006-lb increment to the

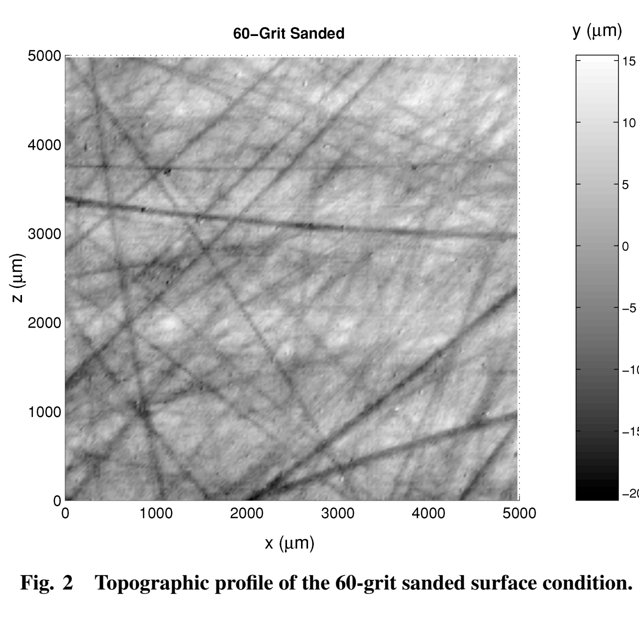

Fig. 2 Topographic profile of the 60-grit sanded surface condition.

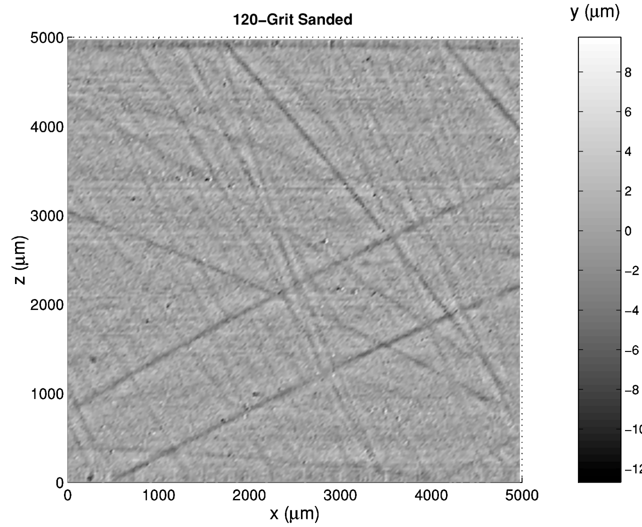

Fig. 3 Topographic profile of the 120-grit sanded surface condition.

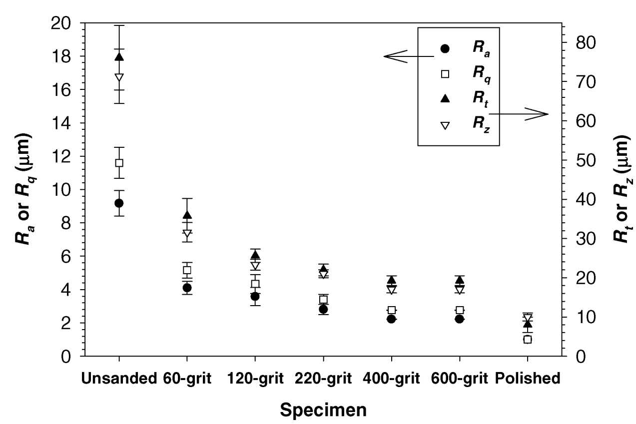

Fig. 4 Roughness plot of the seven surface finish conditions.

drag force, a negligible amount compared to the balance precision. Tunnel blockage accounted for a maximum 1.24–1.39% increase in the freestream velocity (depending on the roughness of the model), which included a constant solid blockage of 5.8%. Streamline curvature corrections shifted the value of α by no more than 0.17–0.20 deg. The value of C_m was likewise shifted by 0.0025–0.0030, depending on the roughness case. Downwash corrections shifted α by an additional 0.96–1.16 deg, with the largest magnitude of shift occurring at the highest values of C_L. The maximum increase in the drag coefficient ranged from 0.0134 to 0.0196. The cumulative effect on wall-interference corrections reduced the maximum L/D ratio by 6.1–7.8%, depending on the roughness case.

Precision uncertainty estimates for the measurements were made through repeatability tests using the procedure given by Moffat.[21] Ten replicate pitch sweeps were made for all of the model surface conditions. The standard error for the mean force coefficients at each angle of attack was calculated. To estimate the 95% precision confidence limits in the mean, its standard error was multiplied by the two-tailed t value ($t = 2.262$) for nine deg of freedom and 95% confidence, as given by Coleman and Steele.[22] These were combined with the estimates of the bias errors to predict the overall 95% confidence limits for C_L, C_D, and C_m. These were estimated to be $\pm 1.0\%$ for C_L, $\pm 2.0\%$ for C_D, and $\pm 6.0\%$ for C_m.

Results And Discussion

The presentation of the results involves discussion of analytic modeling of the baseline configuration, the observed experimental aerodynamic characteristics and implications, and the Reynolds-number effects. These results, obtained for systematically quantified roughness scales not typically reported, confirm the improvements

Table 1 Summary of aerodynamic data, unsanded surface finish

	Reynolds number	
Parameter	5.6×10^5	1.06×10^6
$C_{L_{max}}$	0.843	0.969
a, deg^{-1}	0.0591	0.0600
C_{D_0}	0.0065	0.0071
C_{m_0}	−0.0060	−0.0061
$(L/D)_{max}$	14.27	13.74

Table 2 Summary of aerodynamic data, polished surface finish

	Reynolds number	
Parameter	5.6×10^5	1.06×10^6
$C_{L_{max}}$	0.808	0.822
a, deg^{-1}	0.0590	0.0601
C_{D_0}	0.0066	0.0065
C_{m_0}	−0.0049	−0.0057
$(L/D)_{max}$	14.18	14.23

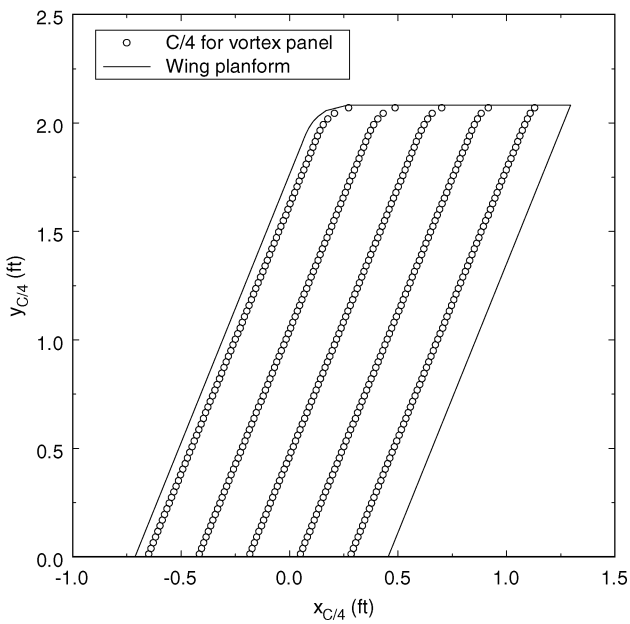

Fig. 5 Panel layout for vortex lattice method.

in stall characteristics that occur as the surface finish becomes rougher. These trends were observed even at the small-scale roughness considered presently (less than 0.46 mils or 11.6 μm rms roughness height). Summaries of the aerodynamic results are listed in Tables 1 and 2.

Vortex Lattice Analysis

Comparisons were made between the baseline experimental results and the vortex lattice method (VLM) of subsonic aerodynamic analysis. VLM is an established method for analyzing complex planar and nonplanar planforms with leading-edge suction and other nonlinear aerodynamic characteristics and has been validated for swept wings.[23,24] The most recent version (VLM Mark 4.997) of Margason and Lamar's original FORTRAN code was used for the present analysis. The stabilizer planform was modeled as a zero-thickness wing using 400 vortex panels: five panels in the chordwise direction and 80 panels in the spanwise direction. The modeled planform is shown with the quarter-chord position of each vortex panel in Fig. 5. Calculations of C_L, C_{D_i}, and C_m were performed for -5 deg $\leq \alpha \leq 20$ deg at a Mach number of 0.1. The analysis represented attached flow with full leading-edge suction everywhere but the outboard 10% of the span. The outboard section is where the leading-edge transitions into the side edge of the wing tip and is treated as a site of separated vortex flow for the purpose of the VLM results. To approximate the total drag of the stabilizer model,

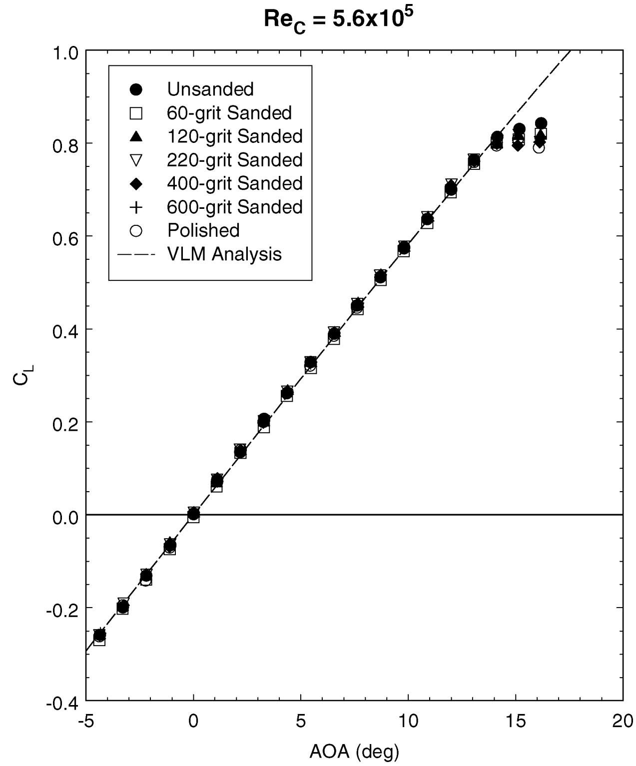

Fig. 6 Lift curves for the lower-Reynolds-number case.

a constant value of the parasite drag ($C_{D_0} = 0.0070$) was added to the VLM-induced drag results. This shifted value was subsequently used in calculations of L/D for the analytic comparisons. Analytic pitching-moment coefficients are referenced to the quarter-chord of the *MAC* of the planform. The VLM results are graphically presented along with the experimental data.

Aerodynamic Characteristics

The most significant effects of surface finish appear as qualitative differences in the stall characteristics of the wing. Furthermore, these differences are accentuated by increasing the Reynolds number. Because no data were taken deep into the stall regime, events leading to stall and the indicators of incipient stall are discussed.

The lift curves demonstrate the differences in the stall characteristics at both Reynolds numbers tested. The experimental lift curves, shown for Reynolds numbers of 5.6×10^5 and 1.06×10^6 in Figs. 6 and 7, compare favorably with the VLM analysis. VLM analysis yielded a constant lift-curve slope of 0.0583 deg^{-1} while the polished stabilizer showed the highest experimental lift-curve slope of 0.0596 deg^{-1} at low angles of attack for both Reynolds numbers. These results show that the experimental results match the analytic C_L values very closely except at angles of attack near the stall angle for the higher Reynolds number. And for the unstalled wings the experimental data are only slightly higher than the analytic C_L calculations. This is likely because of thickness effects, which are unaccounted for in the VLM formulation. At most, this amounts to a difference of $\Delta C_L = 0.04$, or a VLM value that is 4% underpredicted at $\alpha = 16.4$ deg. Despite this deficiency, the VLM results form a valid benchmark for the experimental data and can be assumed to represent idealized aerodynamic trends.

As seen for all experimental surface finishes, there were no significant changes in the lift characteristics (qualitatively or quantitatively) at angles below $\alpha \approx 12$ deg. The value of α_{L_0} remained at zero, and the lift-curve slope was in the range 0.0588–0.0601 deg^{-1}. These observations confirm that the lift is insensitive to the rougher surface finishes at low to moderate angles of attack.

Above 12-deg angle of attack, the trends in lift coefficient become separated to indicate differences in the prestall and stall characteristics of the stabilizer as a function of the surface finish. At both Reynolds numbers the trend is that the rougher surfaces are less

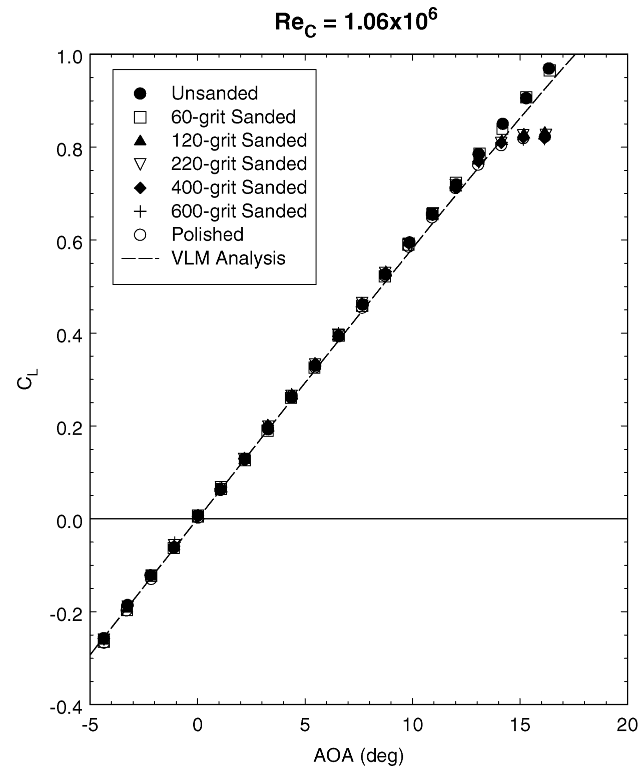

Fig. 7 Lift curves for the higher-Reynolds-number case.

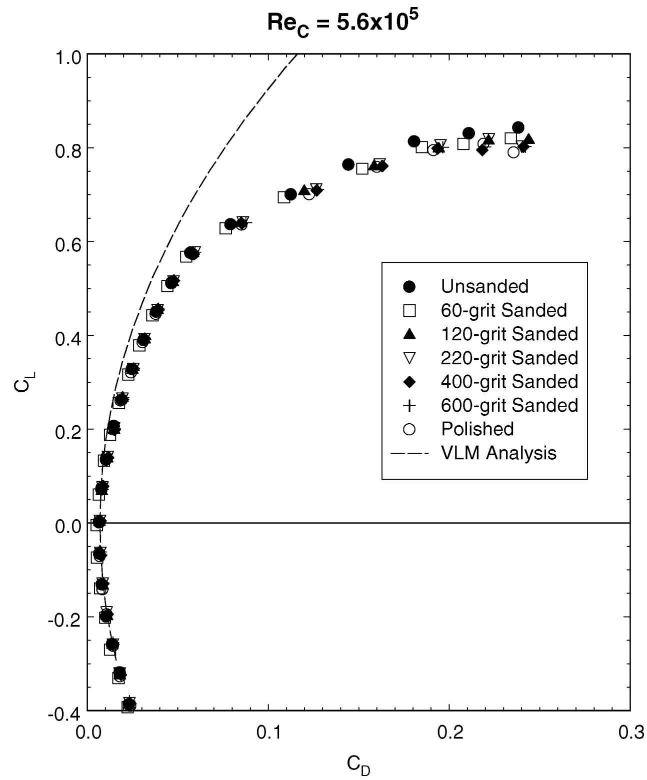

Fig. 8 Drag polars for the lower-Reynolds-number case.

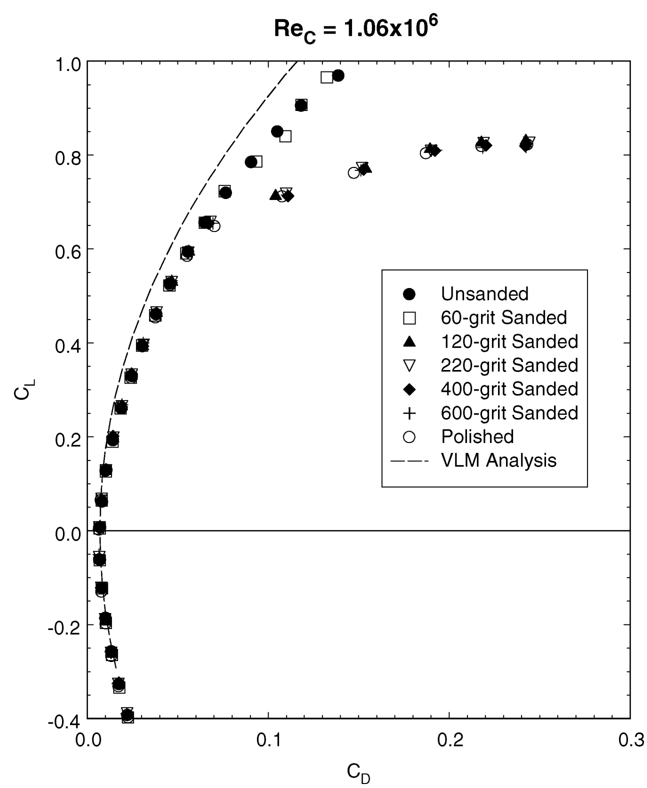

Fig. 9 Drag polars for the higher-Reynolds-number case.

affected by early stall tendencies than are the smoother surfaces, resulting in a smaller deviation from the theoretical linear lift curve. In fact, the two roughest surfaces never achieve a true stall condition because the lift coefficient never achieves its maximum value; it continues to increase with the angle of attack. Therefore, the cases that depart from the linear lift curve but never reach a maximum can be considered to be in the incipient stall regime, but yet unstalled in the strictest sense (i.e., not in the deep-stall regime). These latter cases are still valuable in the analysis, however, because the threshold of true stall occurs as a result of boundary-layer separation in the adverse pressure gradient. More importantly, the unsanded and 60-grit sanded surfaces produced lift coefficients that deviated very little from the linear lift curve trend even at the maximum angle of attack of 16 deg when tested at the higher Reynolds number. This lift data support the conclusion that the presence of rougher surface finishes on the stabilizer partially suppresses boundary-layer separation in an adverse pressure gradient, thus delaying stall to higher angles of attack.

The drag polars, shown in Figs. 8 and 9, also showed qualitative changes as a result of differences in the incipient stall characteristics. Much like the lift results, the drag polars show good agreement for all surface finishes below a lift coefficient of approximately 0.6. In this range the VLM results consistently underpredicted the drag coefficients despite matching the value at zero lift with the experimental data. At a Reynolds number of 5.6×10^5, the VLM drag coefficients were 24–26% below the experimental results. At a Reynolds number of 1.06×10^6, the VLM underpredicted the drag coefficient by only 19–22%. This is a relatively manageable difference considering it is a comparison between viscous flow measurements and an inviscid analysis. The true parasite drag coefficient indeed changes with the angle of attack, generally increasing. Thus, the assumption of a constant offset in the drag polar is imprecise because the contribution of skin friction will increase with angle of attack, but the VLM drag polar presents a reasonable benchmark for the trends in the experimental data.

At zero lift the drag coefficient is independent of the surface finish, to within the measurement precision of the force balance system. For the lower-Reynolds-number runs, the value of C_{D_0} averaged 0.0066 with a standard deviation of ± 0.0007 for all seven surface finishes. The higher-Reynolds-number runs produced an average C_{D_0} of 0.0067 with a standard deviation of ± 0.0002 (which is on the order of measurement precision).

Because the parasitic drag coefficient is insensitive to the surface finish quality, there is a shift in the proportionate contributions to the overall drag. The rougher surfaces doubtless promoted a higher contribution as a result of skin friction. A constant total drag coefficient therefore means that the pressure drag contribution decreased as the surface roughness was increased. This conclusion suggests that the rougher surfaces produced a thinner wake and consequently a lower pressure drag in the vicinity of zero lift.

Above $C_L \approx 0.6$ the increase in drag coefficient was coincident with stall behavior as revealed in the lift-curve data. The advent of stall was manifest in the drag polars as a sharp departure over the idealized VLM results. The two roughest surfaces consistently produced less overall drag than the smoother surfaces at the same Reynolds number. Moreover, the two roughest surface finishes at a Reynolds number of 1.06×10^6 produced the lowest drag overall and showed no evidence of stall or incipient stall. This trend is indicative that the rougher surfaces generated a boundary layer with a higher degree of turbulent characteristics, and the turbulent boundary layer was less likely to separate at higher angles of attack and more adverse pressure gradients. These results are consistent with the observations in the lift curves.

Likewise, pitching moment varied in accordance with the stall characteristics. The pitching-moment coefficients, calculated with respect to the MAC quarter-chord position, are shown in Figs. 10 and 11. Although the data show considerably more scatter than do the lift and drag data, all surface finishes collapse onto a common linear trend for $\alpha < 10$ deg. At a reference angle of $\alpha = 9.9$ deg, the experimental results are 14–19% below the VLM analysis, depending on the surface finish and Reynolds number. The largest contributor to this deviation is the offset in α of approximately 1 deg at the zero pitching-moment coefficient. Because the assumedly symmetric wing was aerodynamically zeroed based on the lift coefficient, any asymmetric aerodynamic effects will appear in the pitching-moment behavior. These model asymmetries are of first-order scale, introduced during the fabrication process, rather than of second-order scale, introduced during the sanding process. The interpolated value of C_{m_0} averages to -0.0054 with a standard deviation of ± 0.0005 for all cases tested, demonstrating an experimental consistency that is within the precision of the instrumentation.

For $\alpha > 10$ deg the moment curve begins to depart from its linear behavior, but C_m still increases with α. For $\alpha > 12$ deg the stall is characterized by a sharp decrease in the pitching moment, which indicates a loss of lift inboard that is supported by analysis. An analysis of the spanwise lift distribution from the vortex lattice calculations suggests that stall initiates at 22% of the wing half-span for the sectional characteristics of the given airfoil. This would result in a loss of lift forward of the aerodynamic center and a net decrease in the pitching-moment coefficient. As the angle of attack increased from 12 to 16 deg, the pitching-moment coefficient decreased sharply from approximately $+0.03$ to -0.03. Past the point of $\alpha \approx 12$ deg, two trends were evident. The five smoothest surfaces followed a trend of lower moment coefficients while the two roughest surfaces followed a trend of higher moment coefficients, a departure emphasized by the nature of the stall.

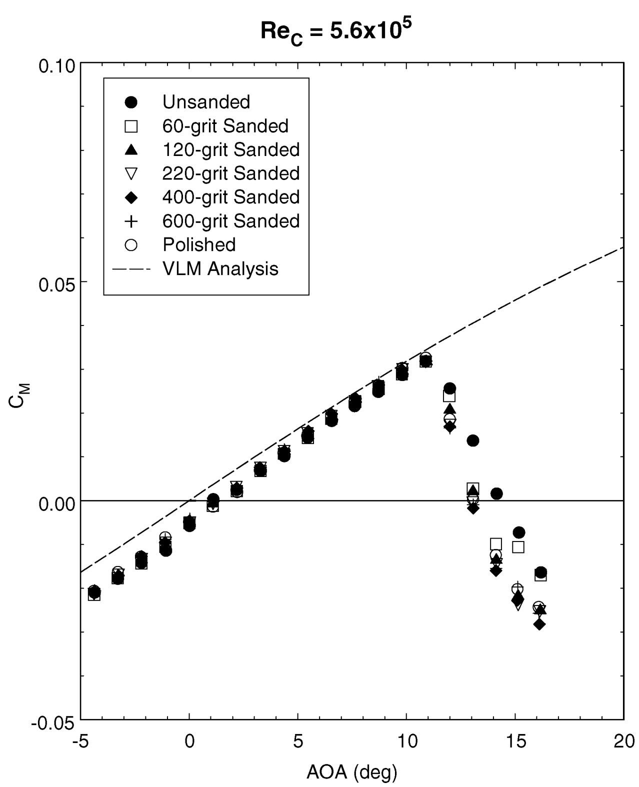

Fig. 10 Pitching-moment coefficients for the lower-Reynolds-number case.

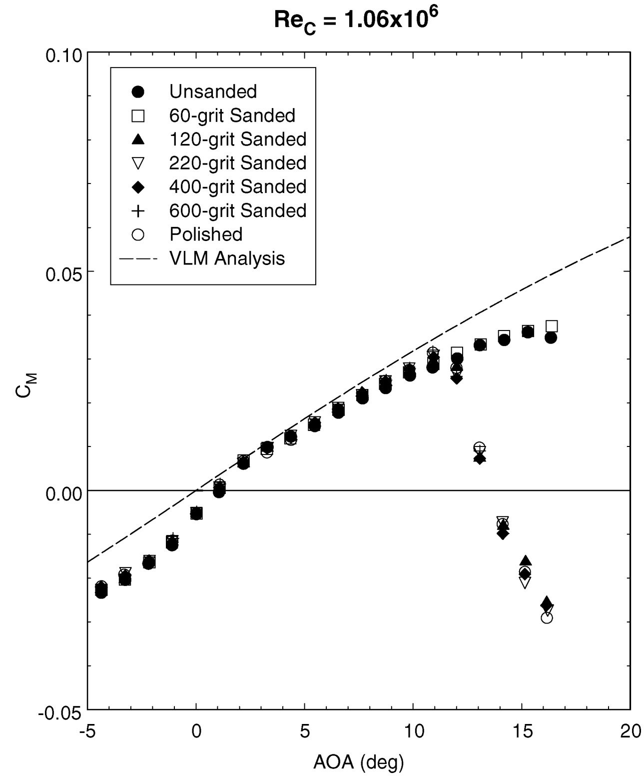

Fig. 11 Pitching-moment coefficients for the higher-Reynolds-number case.

Though the limits in the surface finish quality were represented by the unsanded wing (the roughest surface) and the polished wing, the limits of the aerodynamic performance did not correspond to these cases. The aerodynamic characteristics show a sharp demarcation as a result of a relatively benign decrease in roughness, from the 60-grit sanded surface to the 120-grit sanded surface. Thus, the most significant performance deficits occur between two surfaces that appear very similar to the laser profilometer, as represented by the topographies in Figs. 2 and 3.

Aerodynamic Efficiency

Although the surface finish effects on C_L and C_D were negligible at low angles of attack, the experimental data show clear differences in the lift-to-drag ratio for $0 < \alpha < 5$ deg. At angles of attack above 5 deg and below 10 deg, the L/D data presented in Figs. 12 and 13 show good consistency with varying scatter (3–8%, depending on the Reynolds number). This trend is similar to what was observed in the lift and drag data at low angle of attack: that surface finish had measurable quantitative effects but negligible qualitative effects in this range.

However, there were statistically significant differences in the data at the lower angles of attack, especially at the point of maximum L/D. The magnitude of $(L/D)_{\max}$ varied from 13.4–15.0 (a change of 4–12%) between the seven surface finishes, depending on the Reynolds number. And contrary to the trends observed for C_L and C_D, the polished surfaces tended to produce some of the highest L/D values. At a Reynolds number of 1.06×10^6, the polished wing had the highest peak value of L/D. The maximum L/D consistently

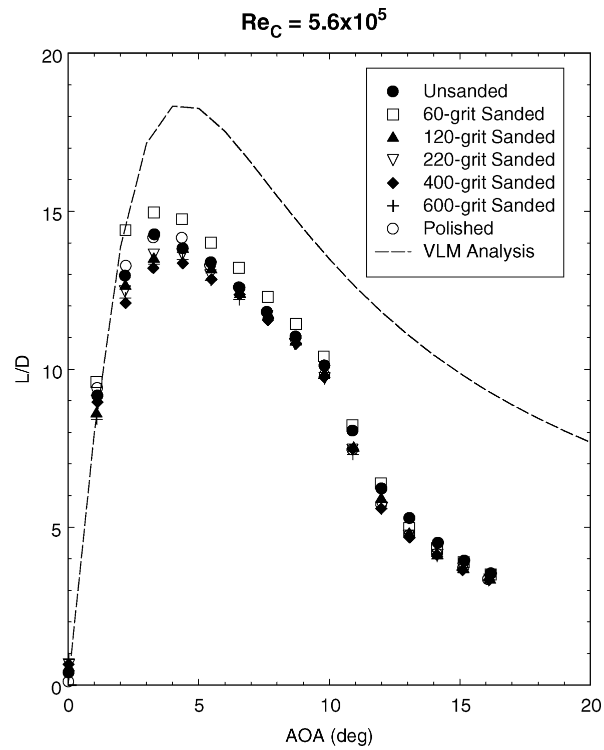

Fig. 12 Aerodynamic efficiencies for the lower-Reynolds-number case.

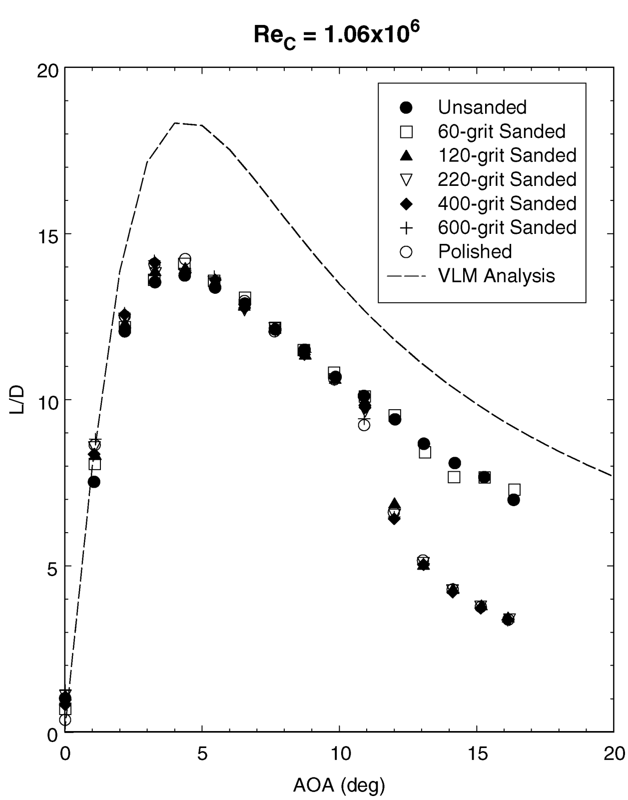

Fig. 13 Aerodynamic efficiencies for the higher-Reynolds-number case.

occurred at an angle of attack of $\alpha \approx 3.5$–4.5 deg. By comparison, the VLM results do a fair prediction of $(L/D)_{\max}$ (18.4) and an excellent prediction of the angle of attack ($\alpha \approx 4$ deg).

To ascertain the presence of any second-order effects caused by the surface roughness, the span efficiency factors were calculated. Span efficiency was calculated by applying an offset parabolic curvefit to the data well outside the prestall regime (nominally $-0.6 < C_L < 0.6$), as presented in the partial drag polars in Figs. 14

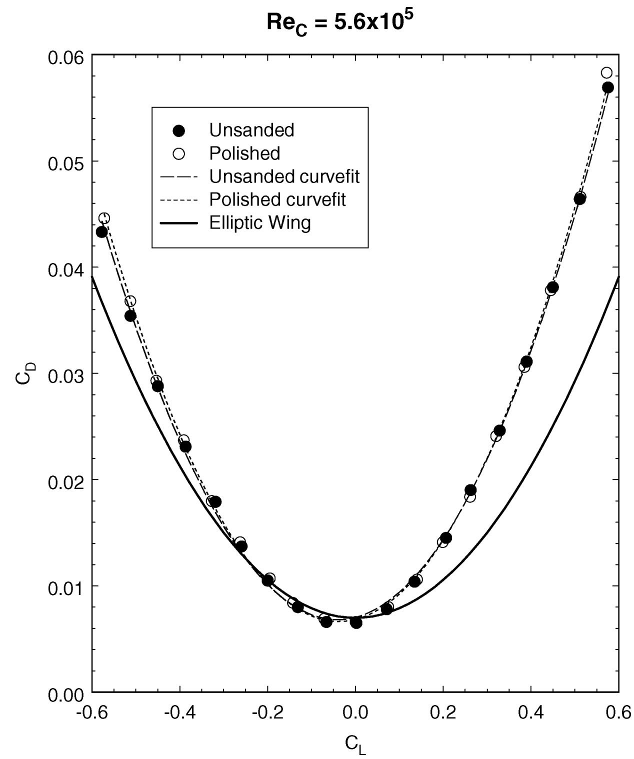

Fig. 14 Drag polar curvefits for the lower-Reynolds-number case.

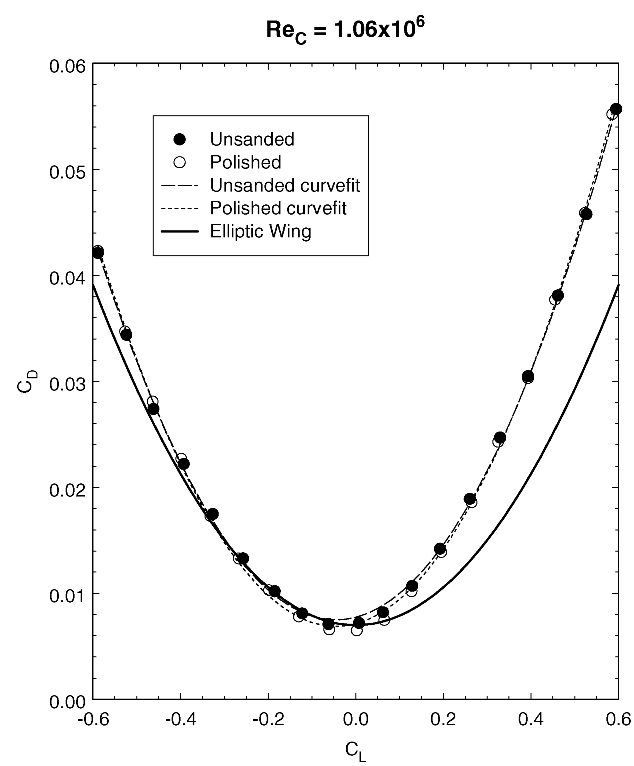

Fig. 15 Drag polar curvefits for the higher-Reynolds-number case.

and 15. The curvefits were achieved with multiple R^2-statistic values in the range 0.9988–0.9991, and the resulting span efficiency factors are presented in Table 3. The results show that the quality of the surface finish affected the value of the span efficiency factor, revealing slight, but consistent differences in the three-dimensional lift distribution. This analysis shows that for the lower Reynolds number e decreased 3.1% from 0.684 to 0.663 as the roughness was decreased from the unsanded to the polished case. At the higher Reynolds number e decreased from 0.755 to 0.733 (a 2.9% reduction) between the unsanded and the polished cases. Although subtle

Table 3 Changes in the span efficiency factor

	Reynolds number	
Surface Finish	5.6×10^5	1.06×10^6
Unsanded	0.684	0.755
Polished	0.663	0.733

decrements the changes indicate that the smoother wing surface was slightly less efficient than the rougher surface with respect to the ideal elliptic lift distribution, despite the obvious reduction in skin-friction coefficient. The data do not reveal any clues concerning the nature of this observation. However, the authors suggest the possibility that the unsanded roughness height was large compared to the boundary-layer thickness such that there was a more effective coupling between the boundary-layer flow and the external flowfield. In so doing, this might have produced more of an elliptic lift distribution. The thicker boundary layer also yields a thicker displacement thickness, which can be a factor in the efficiency of the wing. It must be emphasized, however, that these effects are very small, but measurable and repeatable. For comparison purposes the VLM results yielded a span efficiency factor of 0.842 based on leading-edge separation and tip suction effects on the outer 10% of the semispan.

Reynolds-Number Effects

Significant differences caused by the change in Reynolds number were noted for C_L, C_D, and C_m. The maximum lift coefficient and the lift-curve slope were shown to be higher at the higher Reynolds number. The effect of increasing the Reynolds number from 5.6×10^5 to 1.06×10^6 was to increase the highest $C_{L_{\mathrm{MAX}}}$ from 0.843 to 0.969 (a 15.0% increase). This increase is presented for the roughest surface finish tested, the unsanded case, but the 60-grit sanded case also showed an increase of similar magnitude (a 17.7% increase). Because no clear stall point was observed within the range of measurements at the higher Reynolds number, the peak C_L observed is not necessarily the true $C_{L_{\mathrm{MAX}}}$ for the wing model. Therefore, these results are a conservative representation of how the surface finish affects the stabilizer's stall characteristics.

Although the value of the lift-curve slope was not significantly affected by the surface finish, it increased measurably and consistently at the higher Reynolds number. The differences in lift-curve slope were least pronounced for angles of attack less than 6 deg and most pronounced for angles of attack greater than 9 deg. At 5.5-deg angle of attack, the lift coefficient increased from 0.316 to 0.326 (a 3% increase) as the Reynolds number was increased from 5.6×10^5 to 1.06×10^6. At 9.8-deg angle of attack, the lift coefficient increased 4% from 0.568 to 0.590. The effect of these results is to increase the value of the lift-curve slope by 4.8% by increasing the Reynolds number, thus demonstrating the relative sensitivity of the flow regime studied. These observations occurred most noticeably in the moderate angle of attack range (5 deg $< \alpha <$ 12 deg).

More importantly, the higher Reynolds number tended to magnify the qualitative changes in the stall characteristics as evidenced by the degree of data spread between the seven surface finishes at the higher angles of attack. The largest difference (comparing the unsanded and the polished surfaces) is a net 4.1% change in $C_{L_{\mathrm{MAX}}}$ at a Reynolds number of 5.6×10^5. At a Reynolds number of 1.06×10^6, the largest difference increases to 15.2%. This result demonstrates a much-delayed stall at the higher Reynolds number and supports the qualitative difference in the lift curve, which maintains a nearly linear slope all the way out to $\alpha = 16$ deg for the two roughest surfaces (unsanded and 60-grit sanded) at a Reynolds number of 1.06×10^6. In summary, it is clear that the increased Reynolds number magnifies the degree to which the increased surface roughness results in a higher observed $C_{L_{\mathrm{MAX}}}$ and a delayed stall point of the wing model.

Increasing the Reynolds number had a measurable effect on the drag. Figure 8 shows that at the lower Reynolds number, all data series are qualitatively similar, yet there is a separation in the data. The two roughest cases (unsanded and 60-grit sanded) show quantitative differences from the remaining five cases: for C_L values above 0.6, the rougher cases were lower in drag by as much as 8%. However, at the higher Reynolds number, Fig. 9 shows that the separation becomes large as a result of the delayed stall point. The drag coefficient at the maximum angle of attack for the five smoothest surfaces averages out to 0.2429, and the scatter is small ($\sigma = 0.0008$). This value is 138% higher than the two roughest cases, which have an average drag coefficient of 0.1018 at the same lift coefficient ($C_L = 0.82$). Thus, increasing the Reynolds number by a factor of two greatly enhanced the favorable stall characteristics resulting from roughness effects.

The quantitative differences in the drag polar were least pronounced for C_L values below 0.4 ($\alpha \approx 7$ deg) and most pronounced for C_L values above 0.6 ($\alpha \approx 11$ deg). At 5.5-deg angle of attack, C_D remained essentially constant for the polished wing, 0.0241 to 0.0243, as the Reynolds number was increased from 5.6×10^5 to 1.06×10^6. At 9.8-deg angle of attack, the drag coefficient decreased 5.3% from 0.0583 to 0.0552. This trend demonstrates that increasing the Reynolds number creates a more shallow drag polar, a fact that is supported by the efficiency calculations. A shallower drag polar will result in a lower induced drag component and a higher value of the span efficiency factor. The data in Table 3 show that e increased about 10.5% as the Reynolds number is increased for the both the unsanded and polished models. This result depicts a consistent Reynolds number trend that spans the surface roughness cases.

The Reynolds-number effects on the drag suggest that the rougher surfaces more effectively turbulate the boundary layer, making it more prone to remain attached in the adverse pressure gradients at higher α. The fact that this effect is most prominent at the higher Reynolds number is indicative that the roughness height is sufficiently large in the thinner boundary layer to energize it. Thus, an rms roughness height of 0.20 mils (5 μm) is sufficient to create the observed effects in the lift, drag, and pitching-moment coefficients. For R_q values below 0.17 mils (4.2 μm), the effects are not observed. Therefore, a higher Reynolds number or an increased surface finish roughness would be expected to produce similar effects in a smoother surface (120-grit sanded, 220-grit sanded, etc.).

The Reynolds number exerted qualitative and quantitative effects on the pitching-moment coefficient. At a Reynolds number of 1.06×10^6, the moment curve took on a different characteristic than at a Reynolds number of 5.6×10^5. Around the vicinity of C_{m_0} ($-3 < \alpha < 3$ deg), the slope $\mathrm{d}C_m/\mathrm{d}\alpha$ was distinctly higher than the VLM predictions at the higher Reynolds number, but for $3 < \alpha < 11$ deg the slope was lower. In the region around $\alpha \approx 3$ deg, the data appeared to be in closer agreement with the VLM analysis, resulting in the break point in the curve. This break point is coincident with the rise to maximum L/D. This break in the slope is in contrast to the case for the lower Reynolds number, which appeared to be much more linear in behavior for $-5 < \alpha < 7$ deg. This change in qualitative trends for the unstalled wing is in marked contrast to the other aerodynamic coefficients.

Both Reynolds numbers resulted in a departure from linear behavior in the region around $\alpha \approx 11$ deg. However, the higher-Reynolds-number runs showed a greater degree of departure than did the lower-Reynolds-number runs, especially for the two roughest surface finishes. The unsanded and 60-grit sanded surface finishes showed the same trend revealed in the lift and drag characteristics: they did not stall at the higher Reynolds number. The pitching moment continued to increase in magnitude beyond $\alpha = 11$ deg as a result of the wing being in an unstalled state. The data plotted for both cases show a peak moment coefficient at $\alpha = 15.3$ deg, but the experimental uncertainty creates the possibility for a peak anywhere in the range $\alpha > 14$ deg. At the least it can be concluded for these cases that the moment coefficient is at or near its peak value at the limit of angles of attack tested.

Conclusions

By systematically quantifying the stabilizer surface finish and measuring the impact on aerodynamic performance, the present study confirmed that the primary influence of surface finish was to alter the stall characteristic by affecting the type of boundary-layer separation. This work was accomplished for scales of roughness and surface measurement techniques not typically reported. Because the roughness effects were only observed at higher angles of attack, the values of a, C_{D_0}, and C_{m_0} were relatively unaffected by the surface finish. The lift-curve slope remained approximately 0.060 $\deg^{-1}$ for all configurations. The parasite drag coefficient remained constant at 0.007 within the limits of experimental precision. The zero-lift pitching-moment coefficient also remained statistically constant at -0.006. In particular, the reported constant value of C_{D_0} departs from the archive literature, mainly because the scale of roughness in the present work is at least two orders of magnitude smaller at $R_q/\bar{c} \approx 10^{-5}$.

However, roughness effects were present in the parameters affected by boundary-layer transition and separation. As a consequence, the smoother surfaces performed below the rougher ones. The unsanded stabilizer had a surface finish of 0.46 mils (11.6 μm) and produced the highest observed $C_{L_{\max}}$ of 0.969, whereas the polished stabilizer had a surface finish of 0.04 mils (1.0 μm) and produced the lowest observed $C_{L_{\max}}$ of 0.808. However, the biggest overall difference in performance occurred between the 60-grit and the 120-grit sanded surface when tested at the higher Reynolds number. This represents a decrease in rms roughness height of 0.03 mils (1.0 μm), yet there was a 13.8% decrease in C_L, an 83% increase in C_D, a 167% decrease in C_m, and a 53% decrease in L/D for the smoother stabilizer surface finish at a fixed angle of attack of 16 deg.

These results have a limited application to the operation of similar aircraft stabilizer geometries. Surface finish and roughness effects are most prominent at the higher angles of attack where boundary-layer transition and separation ensues. For conventional vertical stabilizers operation in this regime is extremely uncommon. For conventional horizontal stabilizers operation in the stall regime is primarily a transient phenomenon. Producing stabilizers with rougher surface finishes will generally not impact the aircraft operational envelope.

However, for sailing applications the rougher surface finish on a fixed stabilizer could improve handling. Small sail craft frequently operate with a stalled or nearly stalled centerboard or daggerboard, especially during large changes in heading (i.e., tacks and gybes). Furthermore, a technique of shaking the rudder (rapidly varying the angle of attack over a small range near the critical angle) is commonly used to reestablish attached flow on that control surface when α_{stall} is exceeded during maneuvering. Thus, a rougher surface finish on the stabilizer could actually improve the performance by expanding the operational envelope a few degrees in angle of attack.

Acknowledgments

The authors thank the Technical Support Division at the U.S. Naval Academy for assistance in preparation of the test model. M. P. Schultz also acknowledges the support of this research by the Office of Naval Research through Grant # N00014-02-WR20325. D. S. Miklosovic would like to acknowledge the support of this research by the Naval Academy Research Council under grant N00014-02-WR20135.

References

[1] Abdel-Rahman, A. A., and Chakroun, W. M., "Surface Roughness Effects on Flow over Airfoils," *Wind Engineering*, Vol. 21, No. 3, 1997, pp. 125–137.

[2] Chakroun, W. M., Abdel-Rahman, A. A., and Taylor, R. P., "Effect of Surface Roughness on Flow over a Circular Cylinder and Flapped Aerofoil," *Proceedings of the ASME Fluids Engineering Division Summer Meeting*, Vol. 237, No. 2, 1996, pp. 845–853.

[3] Mueller, T. J., and Batill, S. M., "Experimental Studies of Separation on a Two-Dimensional Airfoil at Low Reynolds Numbers," *AIAA Journal*, Vol. 20, No. 4, 1982, pp. 457–463.

[4] Gregorek, G. M., "Effects of Insect Configuration on Wind Turbine Airfoils," *American Society of Mechanical Engineers, Solar Energy Division (Publication) SED,* Vol. 11, 1991, p. 43.

[5] Reuss, R. L., Gregorek, G. M., and Miklosovic, D. S., "Studies of Wind Turbine Airfoils and Roughness," *American Society of Mechanical Engineers, Solar Energy Division (Publication) SED*, Vol. 12, 1992, p. 17.

[6] Wickens, R. H., and Nguyen, V. D., "Wind Tunnel Investigation of a Wing-Propeller Model Performance Degradation due to Distributed Upper-Surface Roughness and Leading Edge Shape Modification," *Canadian Aeronautics and Space Journal*, Vol. 38, No. 4, 1992, pp. 164–172.

[7] Kind, R. J., Potapczuk, M. G., Feo, A., Golia, C., and Shah, A. D., "Experimental and Computational Simulation of In-Flight Icing Phenomena," *Progress in Aerospace Sciences*, Vol. 34, No. 5–6, 1998, pp. 257–345.

[8] Blair, M. F., "An Experimental Study of Heat Transfer in a Large-Scale Turbine Rotor Passage," *Journal of Turbomachinery*, Vol. 116, No. 1, 1994, pp. 1–13.

[9] Abuaf, N., Bunker, R. S., and Lee, C. P., "Effects of Surface Roughness on Heat Transfer and Aerodynamic Performance of Turbine Airfoils," *Journal of Turbomachinery*, Vol. 120, No. 3, 1998, pp. 522–529.

[10] Nikuradse, J., "Laws of Flow in Rough Pipes," NACA TM 1292, 1933.

[11] Djenidi, L., Elavarasan, R., and Antonia, R. A., "The Turbulent Boundary Layer over Transverse Square Cavities," *Journal of Fluid Mechanics*, Vol. 395, 1999, pp. 271–294.

[12] Perry, A. E., and Li, J. D., "Experimental Support for the Attached-Eddy Hypothesis in Zero-Pressure Gradient Turbulent Boundary Layers," *Journal of Fluid Mechanics*, Vol. 218, 1990, pp. 405–438.

[13] Hama, F. R., "Boundary-Layer Characteristics for Rough and Smooth Surfaces," *Transactions SNAME*, Vol. 62, 1954, pp. 333–351.

[14] Ligrani, P. M., and Moffat, R. J., "Structure of Transitionally Rough and Fully Rough Turbulent Boundary Layers," *Journal of Fluid Mechanics*, Vol. 162, 1986, pp. 69–98.

[15] Krogstad, P. Å., Antonia, R. A., and Browne, L. W. B., "Comparison Between Rough- and Smooth-Wall Turbulent Boundary Layers," *Journal of Fluid Mechanics*, Vol. 245, 1992, pp. 599–617.

[16] Raupach, M. R., Antonia, R. A., and Rajagopalan, S., "Rough-Wall Turbulent Boundary Layers," *Applied Mechanics Review*, Vol. 44, No. 1, 1991, pp. 1–25.

[17] Song, S., and Eaton, J. K., "The Effects of Wall Roughness on the Separated Flow over a Smoothly Contoured Ramp," *Experiments in Fluids*, Vol. 32, No. 7, 2002, pp. 38–46.

[18] Schultz, M. P., "The Relationship Between Frictional Resistance and Roughness for Surfaces Smoothed by Sanding," *Journal of Fluids Engineering*, Vol. 124, No. 2, 2002, pp. 492–499.

[19] Bethwaite, F., *High Performance Sailing*, International Marine, Camden, Maine, 1993, pp. 232–234.

[20] Barlow, J. B., Rae, W. H., and Pope, A., *Low-Speed Wind Tunnel Testing*, 3rd ed., Wiley, New York, 1999, pp. 367–427.

[21] Moffat, R. J., "Describing the Uncertainties in Experimental Results," *Experimental Thermal and Fluid Science*, Vol. 1, Jan. 1988, pp. 3–17.

[22] Coleman, H. W., and Steele, W. G., "Engineering Application of Experimental Uncertainty Analysis," *AIAA Journal*, Vol. 33, No. 10, 1995, pp. 1888–1896.

[23] Lamar, J., and Gloss, B., "Subsonic Aerodynamic Characteristics of Interacting Lifting Surfaces with Separated Flow around Sharp Edges Predicted by a Vortex-Lattice Method," NASA TN D-7921, Sept. 1975.

[24] Margason, R. J., and Lamar, J. E., "Vortex-Lattice FORTRAN Program for Estimating Subsonic Aerodynamic Characteristics of Complex Planforms," NASA TN D-6142, Feb. 1971.